Composites Communications 21 (2020) 100395

Contents lists available at ScienceDirect

Composites Communications

journal homepage: www.elsevier.com/locate/coco

Hierarchical composites of $NiCo_2S_4$ nanorods grown on carbon nanofibers as anodes for high-performance lithium ion batteries

Longsheng Zhang [a], Yunpeng Huang [a], Yue-E Miao [b], Wei Fan [b,*], Tianxi Liu [a,b]

[a] Key Laboratory of Synthetic and Biological Colloids, Ministry of Education, School of Chemical and Material Engineering, Jiangnan University, Wuxi, 214122, China
[b] State Key Laboratory for Modification of Chemical Fibers and Polymer Materials College of Materials Science and Engineering, Innovation Center for Textile Science and Technology, Donghua University, Shanghai, 201620, China

ARTICLE INFO

Keywords:
Lithium ion batteries
Anode materials
Metal sulfides
Carbon nanofibers

ABSTRACT

The increasing requirement for clean energy storage has urged the advancement of lithium ion batteries (LIBs) with high specific capacity and cycling stability. In this work, we report a facile method to synthesize hybrid membranes of $NiCo_2S_4$ nanorod arrays uniformly grown onto each carbon nanofiber ($NiCo_2S_4$/CNF), which as anode materials can achieve high performance for LIBs. The conductive networks of CNFs can facilitate the electron transport at the interfaces and diffusion of ions to readily react with $NiCo_2S_4$, thus leading to increased lithium storage. The CNFs can mitigate the drastic expansion/contraction of $NiCo_2S_4$ nanorods, resulting in enhanced cycling stability. As a consequence, the LIBs with $NiCo_2S_4$/CNF hybrid membranes as anode materials exhibit high capacity (1060 mA h/g) at 0.2 A/g and good durability for 100 cycles.

1. Introduction

The increasing demand of efficient energy storage for electric vehicles and portable electronic devices, has urged the rapid development of high-performance lithium ion batteries (LIBs) [1]. As the commercial anodes for LIBs, graphite exhibits high stability but low specific capacity, which impedes the advancement of LIBs [2–4]. Thus, breakthroughs in seeking for alternative anode materials for LIBs are urgently desired.

With high specific capacity, metal sulfides (e.g. SnS_2, NiS, $NiCo_2S_4$, etc.) recently drew great interests as anodes for LIBs [5–10]. However, the agglomeration of these metal sulfides often results in decreased material utilization and rapid capacity decay [11–13]. Besides, the low electrical conductivity of metal sulfide leads to increased charge transfer resistance [14–16]. Constructing nanostructured composites of metal sulfides and carbonaceous materials was proven to be an effective strategy to address these issues [17–19]. Carbonaceous materials provide conductive contacts to facilitate the charge transport at the interfaces and mitigate the expansion/contraction of metal sulfides upon cycling process [20].

Here, we report a facile approach to synthesize hybrid membrane of $NiCo_2S_4$ nanorod arrays grown on carbon nanofibers ($NiCo_2S_4$/CNF), which can efficiently restrain the rapid capacity decay of $NiCo_2S_4$ and achieve high specific capacity and cycling stability. The three-dimensional (3D) interconnected conductive CNF network facilitates the electron transport during the electrochemical reaction process. Besides, the 3D network structures can enable readily access of lithium ions to $NiCo_2S_4$ nanorods that are uniformly grown on nanofibers. As a consequence, the LIBs with $NiCo_2S_4$/CNF hybrid membranes as binder-free anode materials shows high capacity and good durability.

2. Experimental

Synthesis of $NiCo_2S_4$/CNF composites. The preparation procedure is illustrated in Fig. 1A. CNF membranes were synthesized through electrospinning of PAN solution, followed by carbonization procedure. $NiCo_2S_4$/CNF composites were synthesized by a hydrothermal reaction. Briefly, $Ni(NO_3)_2{\cdot}6H_2O$ (1 mmol), $Co(NO_3)_2{\cdot}6H_2O$ (2 mmol), thiourea (8 mmol) and urea (4 mmol) were dissolved in water (30 mL). The above solution was then poured into a 50 mL autoclave with a piece of CNF membrane added into the mixed solution, which was kept at 160 °C for 12 h. Accordingly, pure $NiCo_2S_4$ was prepared by a similar procedure without adding CNF membrane.

Electrochemical Measurements. $NiCo_2S_4$/CNF membranes were directly utilized as the anodes for LIBs. $NiCo_2S_4$ anodes were prepared by coating slurry (mixture of $NiCo_2S_4$, carbon black and poly(vinylidene fluoride) with weight ratio of 8/1/1) onto copper-foil current collectors.

* Corresponding author.
E-mail address: weifan@dhu.edu.cn (W. Fan).

https://doi.org/10.1016/j.coco.2020.100395
Received 26 May 2020; Received in revised form 5 June 2020; Accepted 5 June 2020
Available online 23 June 2020

After being dried at 60 °C overnight under vacuum, the slurry-coated copper foil was cut into discs, which was then used as anodes for LIBs. Coin cells with $NiCo_2S_4$/CNF and $NiCo_2S_4$ anodes were assembled, with lithium foil cathodes and Celgard-2400 separators. Cyclic voltammetry (CV) were conducted on a CHI660D electrochemical workstation at 0.1 mV/s. The discharge/charge experiments were carried out on a CT2013A instrument.

3. Results and discussions

As shown in Fig. 1A, CNF membrane was prepared *via* electrospinning followed by carbonization, which is an effective technique to prepare carbon nanofibers [21–27]. Then, $NiCo_2S_4$/CNF hybrid membrane was obtained by growing $NiCo_2S_4$ nanorod arrays on CNFs *via* a hydrothermal method. Scanning electron microscopy (SEM) results (Fig. 1B) display that the as-prepared electrospun carbon nanofibers have 3D network structures. The nanofibers of CNF have clean surfaces with diameter of 300–350 nm. As shown in Fig. 1C and D, for the $NiCo_2S_4$/CNF hybrid membrane, $NiCo_2S_4$ nanorod arrays are uniformly grown onto each nanofiber. The transmission electron microscopy (TEM) images in Fig. S1 also verify the nanorod morphology. The d-spacing of (311) plane in $NiCo_2S_4$ nanorods is measured at 2.83 Å. The energy dispersive spectroscope (EDS) spectrum and mapping images (Fig. 2) indicate the homogeneous distribution of Ni, Co, S and C elements within each hybrid nanofibers.

The hierarchical structures of $NiCo_2S_4$/CNF nanocomposites with large surface area can enable readily access of lithium ions to $NiCo_2S_4$, optimizing electrode material utilization. By increasing the feed amount of metal precursors during the preparation procedure, the content of $NiCo_2S_4$ nanorods grown on carbon nanofibers is increased accordingly (Fig. S2). After replacing urea with hexamethylenetetramine during the preparation process, the morphology of $NiCo_2S_4$ will change, resulting in $NiCo_2S_4$ nanosheets grown onto nanofibers (Fig. S3). Without additives used during the preparation procedure, the $NiCo_2S_4$/CNF sample features a morphology of $NiCo_2S_4$ nanoneedles grown onto nanofibers (Fig. S4). In sharp contrast, pure $NiCo_2S_4$ sample features an agglomerated structure with $NiCo_2S_4$ nanorods aggregated with each other (Fig. S5). Constructing hierarchical $NiCo_2S_4$/CNF nanostructures can prevent the aggregation of $NiCo_2S_4$ and buffer the expansion/contraction of $NiCo_2S_4$ upon cycling. The macroporous structures of $NiCo_2S_4$/CNF can enable readily access of lithium ions with $NiCo_2S_4$ nanorods that are uniformly grown on nanofibers (Fig. S6).

X-ray diffraction (XRD) patterns of $NiCo_2S_4$ and $NiCo_2S_4$/CNF composite (Fig. 3A) display same diffraction peaks located at 2θ = 16.7°, 27.1°, 31.9°, 38.6°, 47.7°, 50.8°, 55.6°, 65.4°, 69.6° and 78.5°, which can all be indexed to $NiCo_2S_4$ (JCPDS 20–0782), respectively. Surface electronic structures of $NiCo_2S_4$/CNF composite were further investigated by X-ray photoelectron spectroscopy (XPS) measurements. As seen, the $NiCo_2S_4$/CNF sample contains Ni, Co, S, O and C elements with no impurities (Fig. 3B). The Ni 2p spectrum in Fig. 3C reveals two strong peaks located at 852.8 eV and 870.2 eV, corresponding to Ni $2p_{3/2}$ and Ni $2p_{1/2}$, respectively. Peaks of nickel-oxygen species located at 856.7 eV are observed, which is resulted from the exposure of sample to air. From the Co 2p spectrum (Fig. 3D), two strong peaks at 778.6 eV and 793.6 eV are observed, corresponding to Co $2p_{3/2}$ and Co $2p_{1/2}$, respectively. In the S 2p spectrum (Fig. 3E), the peaks located at 161.4 eV and 162.6 eV are assigned to S $2p_{3/2}$ and S $2p_{1/2}$ orbitals of S^{2-}. These results are in accordance with those of $NiCo_2S_4$ materials [28–30].

We further assembled battery cells with $NiCo_2S_4$/CNF and pure $NiCo_2S_4$ as anodes. The $NiCo_2S_4$/CNF membranes were directly utilized as anodes while $NiCo_2S_4$ anodes were prepared using slurry-coating technique. As shown in Fig. 4A, CV curves of cell assembled with $NiCo_2S_4$/CNF anodes reveal three reduction peaks in the cathodic scans and three oxidation peaks in the anodic scans. The reduction peaks are

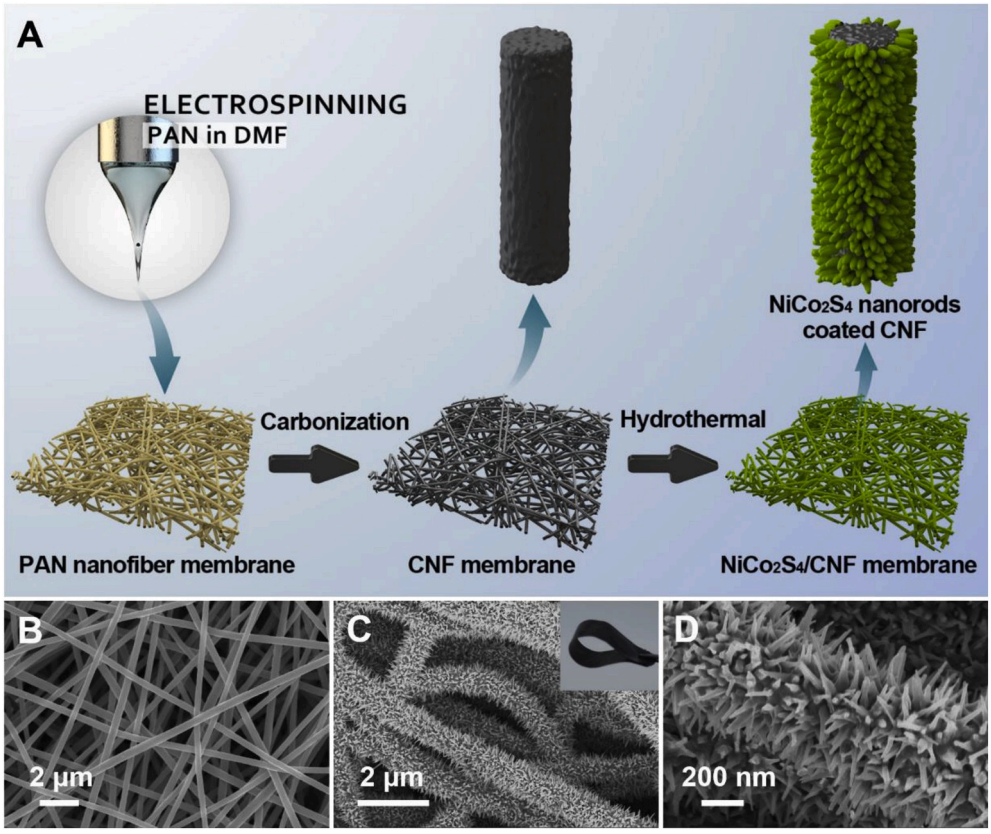

Fig. 1. Schematic of the preparation procedure of $NiCo_2S_4$/CNF hybrid membrane. SEM images of (B) CNF and (C, D) $NiCo_2S_4$/CNF hybrid membranes, respectively. Inset of (C) is the photo of $NiCo_2S_4$/CNF hybrid membrane.

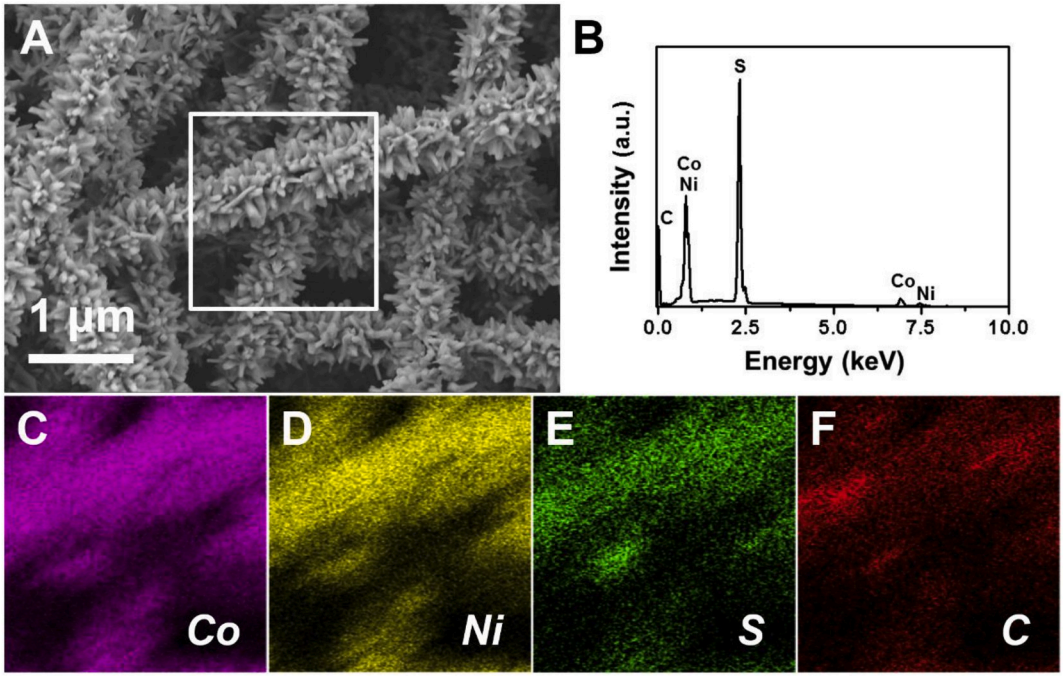

Fig. 2. (A) SEM image, (B–F) corresponding EDS spectrum and mapping images of $NiCo_2S_4$/CNF hybrid membrane, respectively.

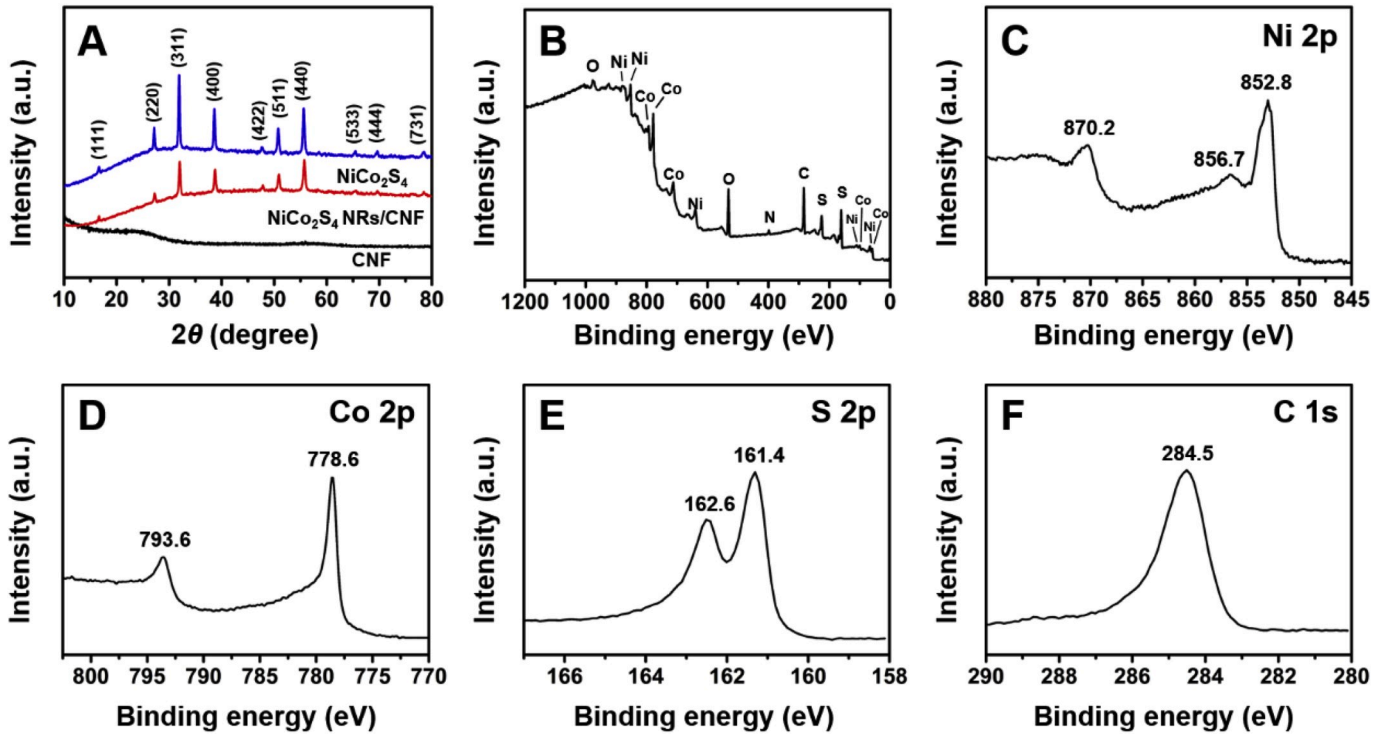

Fig. 3. (A) XRD patterns of CNF, $NiCo_2S_4$ and $NiCo_2S_4$/CNF samples. (B) XPS survey spectrum, high resolution (C) Ni 2p spectrum, (D) Co 2p spectrum, (E) S 2 p spectrum and (F) C 1s spectrum of $NiCo_2S_4$/CNF sample, respectively.

assigned to the reactions between $NiCo_2S_4$ and lithium ions, with products of Ni, Co and Li_2S [14,15]. In the anodic scans, the oxidation peaks are corresponding to the reversible formation of $NiCo_2S_4$. The overlapped CV curves of subsequent cycles suggest good stability of $NiCo_2S_4$/CNF anodes during the reaction process. Fig. 4B shows the discharge/charge curves of cell assembled with $NiCo_2S_4$/CNF anodes. The potential plateaus observed in the discharge and charge curves are consistent with the CV results. The overlapped discharge and charge curves also verify high reversibility of $NiCo_2S_4$/CNF anodes.

We further evaluate the cycling performance of $NiCo_2S_4$ and $NiCo_2S_4$/CNF anodes (Fig. 4C). The cell with $NiCo_2S_4$ anode exhibits poor cycling performance with reversible capacity of 350 mA h/g after 100 cycles, which is possibly resulted from the aggregation and pulverization of $NiCo_2S_4$ that occurred upon cycling. In comparison, the cell assembled with $NiCo_2S_4$/CNF anodes features good cycling stability with a high capacity of 1060 mA h/g. The capacity loss in the initial

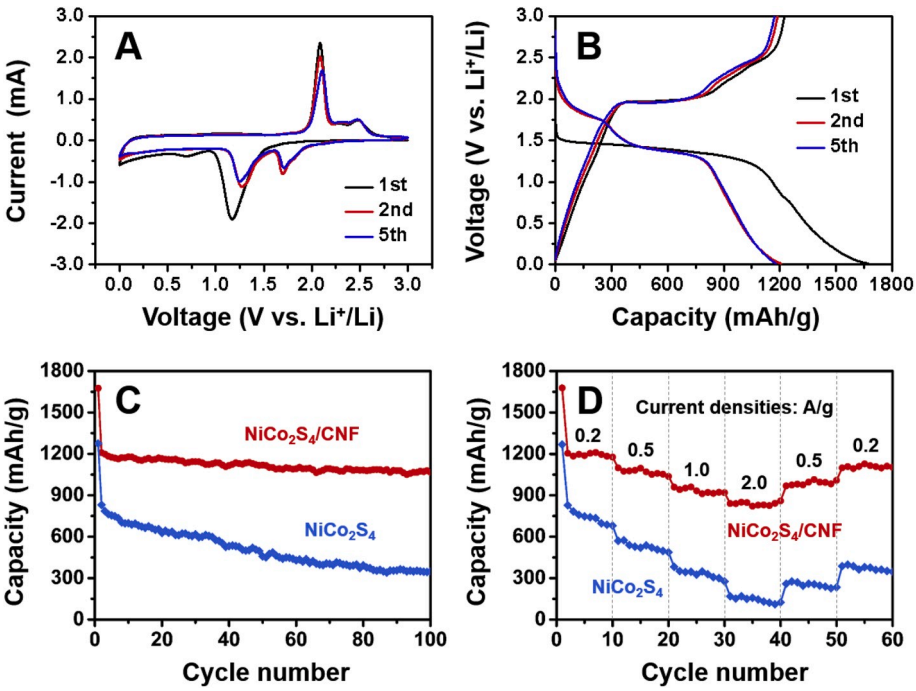

Fig. 4. (A) First three CV curves of cell with $NiCo_2S_4$/CNF anode in the voltage range from 0.01 to 3.0 V at a scan rate of 0.1 mV/s. (B) First three discharge/charge curves of cell with $NiCo_2S_4$/CNF anode. (C) Cycling performance of cells with $NiCo_2S_4$ and $NiCo_2S_4$/CNF anodes at 0.2 A/g. (D) Rate performance of cells with $NiCo_2S_4$ and $NiCo_2S_4$/CNF anodes at various current densities.

cycle are attributed to the formation of solid electrolyte interface layer and dissolution of metal cations [19,20]. Besides, as shown in Fig. 4D, the rate capabilities of $NiCo_2S_4$/CNF anode at various current densities are higher than those of $NiCo_2S_4$ anodes. In conjunction with morphological results, the hierarchical structures of $NiCo_2S_4$/CNF with $NiCo_2S_4$ nanorods grown on conductive carbon nanofibers can enable electrical contact to facilitate the electron transport and diffusion of lithium ions to readily access $NiCo_2S_4$ nanorods, leading to greatly increased lithium storage. The carbon nanofibers can also accommodate the volumetric expansion/contraction of $NiCo_2S_4$ nanorods and mitigate aggregation and pulverization of $NiCo_2S_4$ materials during the cycling process, resulting in improved cycling stability.

4. Conclusions

In summary, we report a facile approach to prepare $NiCo_2S_4$/CNF hybrid membranes with $NiCo_2S_4$ nanorod arrays grown on electrospun carbon nanofibers. The 3D conductive CNF network can enable readily access of lithium ions to $NiCo_2S_4$ nanorods and facilitate the electron transport at the interfaces. As a result, the battery with $NiCo_2S_4$/CNF hybrid membrane as binder-free anode exhibits a high capacity of 1060 mA h/g at 0.2 A/g and good durability. This work provides insights for further advances to design anodes for achieving high-performance LIBs.

Declaration of competing interest

The authors declare that they have no known competing financial interests or personal relationships that could have appeared to influence the work reported in this paper.

CRediT authorship contribution statement

Longsheng Zhang: Methodology, Investigation, Writing - original draft. **Yunpeng Huang:** Investigation. **Yue-E Miao:** Investigation. **Wei Fan:** Supervision, Writing - review & editing. **Tianxi Liu:** Conceptualization, Supervision.

Acknowledgements

The authors are grateful for the financial support from the National Natural Science Foundation of China (21704014), Shanghai Sailing Program (17YF1400200), Shanghai Municipal Education Commission (17CG33), Program of Shanghai Academic Research Leader (17XD1400100), and Shanghai Scientific and Technological Innovation Project (18JC1410600).

Appendix A. Supplementary data

Supplementary data to this article can be found online at https://doi.org/10.1016/j.coco.2020.100395.

References

[1] Y.Y. Liu, Y.Y. Zhu, Y. Cui, Challenges and opportunities towards fast-charging battery materials, Nat. Energy 4 (2019) 540–550, https://doi.org/10.1038/s41560-019-0405-3.
[2] H.T. Sun, J. Zhu, D. Baumann, et al., Hierarchical 3D electrodes for electrochemical energy storage, Nat. Rev. Mater. 4 (2019) 45–60, https://doi.org/10.1038/s41578-018-0069-9.
[3] X.F. Wang, Y.M. Qian, L.N. Wang, et al., Sulfurized polyacrylonitrile cathodes with high compatibility in both ether and carbonate electrolytes for ultrastable lithium–sulfur batteries, Adv. Funct. Mater. 29 (2019) 1902929, https://doi.org/10.1002/adfm.201902929.
[4] G.Y. Zhou, Y.E. Miao, Z.X. Wei, et al., Bio-inspired micro/nanofluidic ion transport channels for organic cathodes in high-rate and ultra-stable lithium/sodium-ion batteries, Adv. Funct. Mater. 28 (2018) 1804629, https://doi.org/10.1002/adfm.201804629.
[5] X.Y. Yu, X.W. Lou, Mixed metal sulfides for electrochemical energy storage and conversion, Adv. Energy Mater. 8 (2018) 1701592, https://doi.org/10.1002/aenm.201701592.
[6] L.S. Zhang, W. Fan, T.X. Liu, Flexible hierarchical membranes of WS_2 nanosheets grown on graphene-wrapped electrospun carbon nanofibers as advanced anodes for highly reversible lithium storage, Nanoscale 8 (2016) 16387–16394, https://doi.org/10.1039/c6nr04241d.
[7] L.S. Zhang, Y.P. Huang, Y.F. Zhang, et al., Three-dimensional nanoporous graphene-carbon nanotube hybrid frameworks for confinement of SnS_2 nanosheets: flexible and binder-free papers with highly reversible lithium storage, ACS Appl. Mater. Interfaces 7 (2015) 27823–27830, https://doi.org/10.1021/acsami.5b09115.

[8] J. Zhou, Y.F. Wang, C. Zhang, Synthesis and electrochemical performance of core-shell $NiCo_2S_4$@nitrogen, sulfur dual-doped carbon composites via confined sulfidation strategy in a polydopamine nanoreactor, Compos. Commun. 12 (2019) 74–79, https://doi.org/10.1016/j.coco.2019.01.001.
[9] X.D. Xu, W. Liu, Y. Kim, et al., Nanostructured transition metal sulfides for lithium ion batteries: progress and challenges, Nano Today 9 (2014) 604–630, https://doi.org/10.1016/j.nantod.2014.09.005.
[10] A.M. Qin, J.Y. Ji, R. Du, et al., Hydrothermal synthesis and electrochemical performance of CuS@Sisal fiber carbon composite Lithium- ion battery anodes, Compos. Commun. 7 (2018) 47–50, https://doi.org/10.1016/j.coco.2017.12.008.
[11] W.W. Yang, L. Chen, J. Yang, et al., One-step growth of 3D $CoNi_2S_4$ nanorods and cross-linked $NiCo_2S_4$ nanosheet arrays on carbon paper as anodes for high-performance lithium ion batteries, Chem. Commun. 52 (2016) 5258–5261, https://doi.org/10.1039/c5cc10368a.
[12] S.Y. Khoo, J.W. Miao, H.B. Yang, et al., One-step hydrothermal tailoring of $NiCo_2S_4$ nanostructures on conducting oxide substrates as an efficient counter electrode in dye-sensitized solar cells, Adv. Mater. Interfaces 2 (2015) 1500384, https://doi.org/10.1002/admi.201500384.
[13] D.X. Bai, F. Wang, J.M. Lv, et al., Triple-confined well-dispersed bioactive $NiCo_2S_4$/$Ni_{0.96}S$ on graphene aerogel for high-efficiency lithium storage, ACS Appl. Mater. Interfaces 8 (2016) 32853–32861, https://doi.org/10.1021/acsami.6b11389.
[14] X.Y. Wu, S.M. Li, B. Wang, et al., $NiCo_2S_4$ nanotube arrays grown on flexible nitrogen-doped carbon foams as three-dimensional binder-free integrated anodes for high-performance lithium-ion batteries, Phys. Chem. Chem. Phys. 18 (2016) 4505–4512, https://doi.org/10.1039/c5cp07541f.
[15] J.G. Wang, D.D. Jin, R. Zhou, et al., One-step synthesis of $NiCo_2S_4$ ultrathin nanosheets on conductive substrates as advanced electrodes for high-efficient energy storage, J. Power Sources 306 (2016) 100–106, https://doi.org/10.1016/j.jpowsour.2015.12.014.
[16] Y.M. Fan, Y.C. Liu, X.B. Liu, et al., Hierarchical porous $NiCo_2S_4$-rGO composites for high-performance supercapacitors, Electrochim. Acta 249 (2017) 1–8, https://doi.org/10.1016/j.electacta.2017.07.175.
[17] L.S. Zhang, L.Z. Zuo, W. Fan, et al., $NiCo_2S_4$ nanosheets grown on 3D networks of nitrogen-doped graphene/carbon nanotubes: advanced anode materials for lithium-ion batteries, ChemElectroChem 3 (2016) 1384–1391, https://doi.org/10.1002/celc.201600183.
[18] D.X. Yuan, G. Huang, D.M. Yin, et al., Metal-organic framework template synthesis of $NiCo_2S_4$@C encapsulated in hollow nitrogen-doped carbon cubes with enhanced electrochemical performance for lithium storage, ACS Appl. Mater. Interfaces 9 (2017) 18178–18186, https://doi.org/10.1021/acsami.7b02176.
[19] X.Y. Wu, S.M. Li, B. Wang, et al., In situ template synthesis of hollow nanospheres assembled from $NiCo_2S_4$@C ultrathin nanosheets with high electrochemical activities for lithium storage and ORR catalysis, Phys. Chem. Chem. Phys. 19 (2017) 11554–11562, https://doi.org/10.1039/c7cp00509a.
[20] S.J. Li, P. Ge, F. Jiang, et al., The advance of nickel-cobalt-sulfide as ultra-fast/high sodium storage materials: the influences of morphology structure, phase evolution and interface property, Energy Storage Mater. 16 (2019) 267–280, https://doi.org/10.1016/j.ensm.2018.06.006.
[21] W. Weng, R. Kurihara, J. Wang, et al., Electrospun carbon nanofiber-based composites for lithium-ion batteries: structure optimization towards high performance, Compos. Commun. 15 (2019) 135–148, https://doi.org/10.1016/j.coco.2019.07.005.
[22] L.L. Wang, F. Liu, W.L. Shao, et al., Graphite oxide dopping polyimide nanofiber membrane via electrospinning for high performance lithium-ion batteries, Compos. Commun. 16 (2019) 150–157, https://doi.org/10.1016/j.coco.2019.09.004.
[23] L.S. Zhang, Y.P. Huang, Y.F. Zhang, et al., Flexible electrospun carbon nanofiber@NiS core/sheath hybrid membranes as binder-free anodes for highly reversible lithium storage, Adv. Mater. Interfaces 3 (2016) 1500467, https://doi.org/10.1002/admi.201500467.
[24] L.S. Zhang, Q.W. Ding, Y.P. Huang, et al., Flexible hybrid membranes with $Ni(OH)_2$ nanoplatelets vertically grown on electrospun carbon nanofibers for high-performance supercapacitors, ACS Appl. Mater. Interfaces 7 (2015) 22669–22677, https://doi.org/10.1021/acsami.5b07528.
[25] Y.E. Miao, G.N. Zhu, H.Q. Hou, et al., Electrospun polyimide nanofiber-based nonwoven separators for lithium-ion batteries, J. Power Sources 226 (2013) 82–86, https://doi.org/10.1016/j.jpowsour.2012.10.027.
[26] W. Ye, J. Zhu, X.J. Liao, et al., Hierarchical three-dimensional micro/nano-architecture of polyaniline nanowires wrapped-on polyimide nanofibers for high performance lithium-ion battery separators, J. Power Sources 299 (2015) 417–424, https://doi.org/10.1016/j.jpowsour.2015.09.037.
[27] Y.C. Ding, H.Q. Hou, Y. Zhao, et al., Electrospun polyimide nanofibers and their applications, Prog. Polym. Sci. 61 (2016) 67–103, https://doi.org/10.1016/j.progpolymsci.2016.06.006.
[28] Y.F. Yuan, L.W. Ye, D. Zhang, et al., $NiCo_2S_4$ multi-shelled hollow polyhedrons as high-performance anode materials for lithium-ion batteries, Electrochim. Acta 299 (2019) 289–297, https://doi.org/10.1016/j.electacta.2019.01.025.
[29] Z.G. Zhang, X. Huang, H. Li, et al., 3-D honeycomb $NiCo_2S_4$ with high electrochemical performance used for supercapacitor electrodes, Appl. Surf. Sci. 400 (2017) 238–244, https://doi.org/10.1016/j.apsusc.2016.12.206.
[30] Y. Song, Z.L. Chen, Y.M. Li, et al., Pseudocapacitance-tuned high-rate and long-term cyclability of $NiCo_2S_4$ hexagonal nanosheets prepared by vapor transformation for lithium storage, J. Mater. Chem. A 5 (2017) 9022–9031, https://doi.org/10.1039/c7ta01758h.